

Research paper

Characterization and workplace exposure assessment of nanomaterial released from a carbon nanotube-enabled anti-corrosive coating

Jonathon A. Brame^a, Erik M. Alberts^{b,*}, Mary K. Schubauer-Berigan^c, Kevin H. Dunn^d, Kelsey R. Babik^c, Eftihia Barnes^e, Robert Moser^e, Aimee R. Poda^a, Alan J. Kennedy^a

^a US Army Engineer Research & Development Center, Environmental Laboratory, United States of America

^b HX5, LLC, United States of America

^c National Institute for Occupational Safety and Health, Division of Surveillance, Hazard Evaluations, and Field Studies, United States of America

^d National Institute for Occupational Safety and Health, Division of Applied Research and Technology, United States of America

^e US Army Engineer Research & Development Center, Geotechnical & Structures Laboratory, United States of America



ARTICLE INFO

Keywords:

Nanomaterial
Coatings
Release
Carbon nanotube
Weathering
Occupational exposure

ABSTRACT

Improvement of methods to quantify the release and characterization of engineered nanomaterials (ENMs) from nano-enabled products is essential to enhance the accuracy and usability of environmental health and safety evaluations. An anticorrosive coating containing multi-wall carbon nanotubes (MWCNTs) was analyzed for nano-scale material and workplace exposure potential. Worker breathing zone measurements for elemental carbon (EC) and electron-microscopy-based structure counts showed negligible MWCNT exposure to workers during laboratory and spray-painting operations over the course of two 8-hour shifts (arithmetic mean inhalable EC and electron microscopy structure count concentrations were 6.47 $\mu\text{g}/\text{m}^3$ and 0.084 structures/ cm^3 respectively). UV weathering prior to abrasion testing increased the nano-size fraction of released material as measured by a fast mobility particle sizer (FMPS) and visual inspection by SEM indicated increased presence of exposed MWCNTs embedded in the polymer matrix. However, no free MWCNTs were identified, despite evidence of MWCNTs embedded in airborne particles. TiO_2 , used as a pigment in the coating and not anticipated as a candidate for nano-specific scrutiny, contained a small fraction (3.5% in number) of nano-sized constituents (< 100 nm). This work emphasizes need for rigorous characterization of additive materials to properly assess potential health hazards and to better our understanding of what qualifies as “nano”.

1. Introduction

The use of engineered nanomaterials (ENMs) in consumer products continues to increase due to their unique, size-dependent properties such as strength, conductivity, surface area, catalytic and photocatalytic capabilities, as well as antimicrobial, magnetic and optical properties (Qu et al., 2012). Applications research and ENM integration into products has outpaced regulatory guidance on potential environmental health and safety (EHS) concerns associated with nanotechnology (Roco, 2011; Collier et al., 2015). The lack of clear EHS assessment guidelines for ENMs and nano-enabled products may result in: (1) overly conservative precautions that unnecessarily slow deployment of novel technologies or (2) inadequate precautions that allow unsafe products to enter the marketplace leading to potential occupational, consumer, and environmental risks. While there is a growing body of work in understanding the hazards of ENM exposure,

there are no formal standards for evaluating ENM release (Petersen et al., 2011; Nowack et al., 2013; Harper et al., 2015; Koivisto et al., 2017) related to exposure potential. Previous evaluations of ENM release have utilized best-available, standardized methods of machining (drilling, grinding, sanding) and weathering (UV exposure) (Froggett et al., 2014; Kingston et al., 2014). These studies have yielded varied results due to differences in sampling and experimental setup, and how these methods reflect on real-world situations remains largely untested. In order to have robust risk guidelines for the use of ENMs, it is vital to have a correlative assessment of release and exposure.

Multi-walled carbon nanotubes (MWCNT) in particular are increasingly being used as additives to polymer matrices to improve properties such as strength and conductivity in many applications from automotive to textiles (Kingston et al., 2014). The inhalation hazards of free CNTs has been studied in previous literature, with results showing effects such as pulmonary inflammation to have dependence on

* Corresponding author at: 3909 Halls Ferry Rd, Vicksburg, MS 39180, United States of America.

E-mail address: Erik.M.Alberts@usace.army.mil (E.M. Alberts).

<https://doi.org/10.1016/j.impact.2018.10.002>

Received 31 May 2018; Received in revised form 7 September 2018; Accepted 23 October 2018

Available online 01 November 2018

2452-0748/© 2018 Elsevier B.V. All rights reserved.

whether the CNTs are single or multi-walled, as well on the aspect ratio of the CNTs themselves (Kuempel et al., 2017; Kobayashi et al., 2017; Wick et al., 2011). A study by Poland et al. (2008) related the pathway of MWCNTs in the body to be similar to asbestos, and inhalation of MWCNTs has induced malignant mesothelioma in mice (Takagi et al., 2008; Fukushima et al., 2018). It should be noted that currently, the understanding of CNT carcinogenicity in humans is limited, and as such the International Agency for Research on Cancer (IARC) classifies all CNTs as group 3 (not classifiable as a carcinogen), with the exception of MWCNT-7, classified as group 2B (possible carcinogen in humans) (IARC, 2017). Additional health hazards of CNTs can include fibrosis, oxidative stress, and genotoxicity (Kuempel et al., 2017; Møller and Jacobsen, 2017).

Recent studies have examined MWCNTs as they are released from polymer matrices; however, the observation of free MWCNTs compared to matrix-bound MWCNTs has been inconsistent due to the variations in method of release and detection (Nowack et al., 2013; Huang et al., 2012; Gohler et al., 2013). Schlagenhauf et al. (2015) utilized MWCNTs pre-labeled with lead ions to detect free MWCNTs in material subjected to abrasion. This study successfully identified free MWCNTs in the inhalable fraction ($< 100 \mu\text{m}$) of the abraded material, however there is some dependency on the abrasion method used and how well MWCNTs are dispersed within the matrix. A recent study by Bishop et al. (2017) did not detect free MWCNT in dust produced by sanding nanotube-containing composites, but found that increasing MWCNT concentration (0.15%–3% by mass) shifted the particle size distribution, indicating greater fractional release of particles in the nanosize range. The properties of the polymer matrix within which the MWCNTs are incorporated also may impact release, such how the polymer deforms around embedded MWCNTs due to deformation and fracture by mechanical stress. Softer polymers such as polyurethane or polyamide show greater resistance to free ENM release vs. harder, more brittle epoxies (Kingston et al., 2014). Along with mechanical stress, chemical or UV weathering susceptibility also impacts free ENM release (Kingston et al., 2014). Meanwhile, additives or surface functionalization of ENMs can inhibit ENM release from susceptible composites (Hirth et al., 2013; Kaiser et al., 2014).

In the present work we focus on characterizing the potential for nano-release from a coating that incorporates two active ingredients for anti-corrosion properties: multi-walled carbon nanotubes and micron-sized zinc (Zn), in addition to a standard titanium dioxide (TiO_2) pigment. Addition of the MWCNTs allows a significant reduction in zinc loading, an environmental risk benefit, but allows the coating to retain anti-corrosion properties. However the addition of MWCNTs may yield a new set of environmental risks. This investigation focuses on characterization of release and exposure potential from an ENM-enabled material during activities related to development, application, and intended use. In particular, exposure potential of ENMs from matrix-bound material is less addressed in the literature relative to hazard and fate (Froggett et al., 2014; Kingston et al., 2014; Hirth et al., 2013; Brame et al., 2015; Peterson et al., 2015). Results are presented on the characterization of the initial material, evaluation of relevant release tests and the results of those release tests throughout the intended use (application and removal), as well as exposure monitoring data for workers involved in typical tasks with the materials.

2. Materials and methods

2.1. Description of anti-corrosive coating and raw materials characterization

Anti-corrosive coating was provided by Tesla Nanocoatings Inc. as a two-part coating (primer and top-coat pigmented with TiO_2) utilizing multi-walled carbon nanotubes (MWCNTs) and micron-scale zinc particles to enhance anti-corrosive properties. Four different sample types were provided by the manufacturer: samples with no coating (sand-

blasted, steel coupon); samples with a MWCNT-containing primer only; samples with the MWCNT-containing primer and a pigmented, non-MWCNT-containing topcoat; and samples with the MWCNT-containing primer and a pigmented, MWCNT-containing topcoat. This sample matrix enabled isolation of the various components to act as comparative controls for release tests. Additionally, the manufacturer provided a dry, un-mixed sample of the primer that was used for additional characterization. Specific information on the zinc and MWCNT components was not made available by the manufacturer.

SEM measurements were carried out with a FEI Nova NanoSEM 630 Field Emission scanning electron microscope using both a backscatter electron (BSE) and a secondary electron (SE) detector with accelerating voltages between 5 kV and 10 kV and spot sizes between 3.0 and 5.0. In order to minimize surface charging, larger samples were coated with a thin layer of gold ($< 5 \text{ nm}$). SEM was also used for particle size measurements of TiO_2 exposed on the surface. Strips of coating were removed from the coated panels with a razorblade and analyzed by SEM at $100,000\times$ resolution. A total of 8 images were analyzed totaling 482 particles using ImagePro (v7, Media Cybernetics Inc., Bethesda, MD). As TiO_2 particles are not perfect spheres, size was measured across the shortest diameter.

Presence of MWCNTs was confirmed by Raman spectroscopy. Spectra were collected using a confocal Raman microscope (Horiba XploRA) equipped with a 600 lines/mm grating. In order to minimize fluorescence signal, a 785 nm excitation laser was used as the Raman excitation source. Briefly, the excitation light was focused on the surface of the samples with a $100\times/0.9 \text{ NA}$ objective, yielding an estimated spot size of $1 \mu\text{m}$. All spectra were acquired with the laser power set to $30 \mu\text{W}$, or less, and the collection time was varied between 60 and 180 s. Prior to collecting spectra from the samples, the instrument was calibrated to the first order Raman peak of silicon (520.6 cm^{-1}). In order to aid in the visualization of the Raman peaks, the collected spectra were plotted after removal of a broad fluorescent background.

2.2. NIOSH workplace-exposure study

Workplace exposure assessment was conducted at Tesla Nanocoatings in Massillon, Ohio. Four volunteer employees provided written consent to be in the study (NIOSH IRB protocol 16-DSHEFS-02XP) and were monitored over a period of two full work days (approximately 8 h each) for exposure to elemental carbon (EC), a marker for CNT exposure, and transmission electron microscopy (TEM)-based structure count concentrations during the manufacture, application and destructive testing of the MWCNT-containing coating. Personal breathing zone (PBZ) and area filter-based air samples (AS) were collected for EC and TEM analysis to assess exposures during the survey. Three PBZ samples were collected on each volunteer (for inhalable EC, respirable EC, and TEM analysis) while area samples (also for inhalable EC, respirable EC, and TEM analysis) were placed at stationary locations throughout the plant to assess task-specific and general workplace air concentrations and potential for migration to non-production areas. These areas included a conference room, a front office, a break room, a high bay area (near spray booth), and in a lab area (along back wall near hood where raw MWCNTs were handled).

Airborne respirable EC was monitored using 25-millimeter (mm) diameter cassettes with quartz fiber filters (QFFs) attached to GK 2.69 BGI cyclones (BGI Inc., Waltham, MA) and connected to Airchek XR5000 sampling pumps (SKC, Inc., Eighty Four, PA) set at 4.2 lpm. Airborne inhalable EC samples were collected using open-faced, 25-mm diameter cassettes with QFFs connected to Leland Legacy sampling pumps (SKC, Inc., Eighty Four, PA) set at 5.0 lpm. The EC samples were analyzed for airborne mass of EC in accordance with NIOSH Manual of Analytical Methods (NMAM) 5040, Diesel Particulate Matter (as Elemental Carbon). To acquire the most accurate representation of the potential exposure workers could experience during a full shift of work at the facility, the EC sample concentration and the background-

corrected eight-hour time weighted average (8-h TWA) were calculated for each of the QFF-based samples collected during the time work was conducted (i.e., the total time pumps were on workers, excluding time workers left the facility for off-site lunch, at which point the pumps were turned off). Since there may be other sources of elemental carbon in the workplace that could interfere in the determination of MWCNT and carbon nanofiber (CNF) exposures, TEM samples were used to assist in characterizing exposures. Studies have shown that airborne background (environmental and in non-process areas in the workplace) concentrations to elemental carbon are typically $< 1 \mu\text{g}/\text{m}^3$ and that an exposure to elemental carbon in the workplace above this level is the best available indicator of CNT or CNF exposure (Evans et al., 2015; Birch et al., 2011a, 2011b; Dahm et al., 2012).

Air samples for transmission electron microscopy (TEM) analysis were collected on 25-mm mixed cellulose ester filters using Airchek XR5000 sampling pumps operating at 4 lpm and analyzed in accordance with a modified NMAM 7402, Asbestos by TEM (NIOSH, 2017). Modifications to NMAM 7402 relate primarily to counting CNT and CNF particles, rather than asbestos fibers. Modifications consisted of eliminating (i) the steps required for asbestos identification and (ii) the requirement that counted particles have diameters $> 0.25 \mu\text{m}$ and meet the traditional definition of a fiber (aspect ratio $\geq 3:1$, longer than $5 \mu\text{m}$). Three 3-mm copper TEM grids prepared from each sample were first examined at low magnification to determine the filter loading and preparation quality. A total of 40 openings were examined at high magnification and any particles containing MWCNT or CNF were counted as MWCNT or CNF 'structures', which ranged from single-fiber MWCNT or CNF to various sized agglomerates comprised of many single MWCNT or CNF fibers. All structures, agglomerated or single fibers, were counted as one 'MWCNT or CNF structure'. Based on the number of MWCNT or CNF structures counted, and the collected air volume, MWCNT or CNF structures per cm^3 were calculated. TEM analysis provides visual evidence of MWCNTs in air, as well as an indication of the structure (i.e., general size, shape and degree of agglomeration) of the collected particles (Dahm et al., 2015).

2.3. Release testing of weathered paint in a sanding chamber

A combinational release testing scenario of accelerated weathering followed by mechanical abrasion was selected based on relevant in-use and end of life (removal) scenarios based on previously described principles (Collier et al., 2015). This method utilized a multi-criteria decision tool (<https://nano.el.erc.dren.mil/tools.html>) to down select from a larger suite of potential release tests based on the intended use of the product, relevance, magnitude of release, time, cost and expertise required to perform each test. Based on this analysis (see Supporting information, Fig. S1), mechanical and UV weathering were chosen as the primary intended-use release tests, and experiments were performed to simulate aggressive mechanical release both with and without prior UV weathering via sanding.

Accelerated weathering was performed using an Atlas UV-weathering system (Atlas Suntest XLS+, Atlas Materials Testing Solutions), which simulated continuous sunlight exposure with a daylight filter (300–400 nm) for 4 weeks (672 h), with a total dose of $145 \text{ MJ}/\text{m}^2$ (Martin et al., 2016). This accelerated weathering protocol used an equivalent to the 1.8 times the solar irradiance at noon on the summer solstice at 40.95°N latitude, near to the latitude of the Tesla Nano-Coatings facility in Massillon, Ohio over a continuous period of 4 weeks to simulate worst-case maximum exposure over 43.6 days in real time.

The custom abrasion chamber was a modification of the Taber Abraser concept, with a rotating sample base and a stationary sanding element with adjustable normal force (Fig. 1A). The abrasion took place within an isolated cabinet with an outlet leading to the instrumentation suite and an inlet creating overpressure to ensure that exterior particles do not contaminate the measurement. The instrumentation suite included a condensation particle counter (CPC; TSI 3007) to measure

total particles $< 1 \mu\text{m}$, a fast mobility particle sizer (FMPS, TSI 3091) to measure particle size distribution from 5.6 nm to 560 nm, and two ports for pump-assisted filters to collect samples for later analysis by scanning electron microscopy (SEM). CPC data was only collected to confirm abrasion produced measurable particles above the background noise and are not included in this report.

Elemental analysis of samples collected from the filters was carried out in conjunction with SEM measurements (as described above), using a Bruker AXS energy dispersive X-ray spectrometer (EDS). The EDS measurements were performed at an accelerating voltage of 15 kV, at a working distance of 5.5 to 6 mm, and a spot size of 5.0 nm. Elemental maps were acquired using a Bruker Esprit EDS detector and analysis software with data analyzed by "precision" tolerances. Elemental maps were acquired only for identified elements of interest (i.e., Zn and/or Ti). MWCNTs presence in the abraded material was again confirmed by Raman spectroscopy as described in the raw materials characterization section.

3. Results

3.1. Raw material characterization

Characterization of the material included SEM and Raman spectroscopy to confirm the presence of the nominal active ingredient materials (MWCNTs and zinc) and assess particle size to determine if the primary particle or fiber diameter merits nano-specific consideration (particles $< 100 \text{ nm}$ in at least one dimension). Both SEM and Raman (Fig. 2) confirmed the presence of CNTs in the raw (powdered) material and the coated primer material and MWCNT topcoat, with width $< 100 \text{ nm}$ and lengths of several hundred nanometers (Fig. 2A). The Raman peaks associated with MWCNTs (D, G and G' peaks) are labeled in Fig. 2B and are in agreement with previous Raman studies (Lehman et al., 2011; Bokobza et al., 2015).

The manufacturer identified micron-sized zinc, used as a sacrificial anode to delay corrosion, as a component of the primer material. Size analysis of the zinc by SEM (Fig. 2C) revealed particles $> 500 \text{ nm}$, significantly larger than the 100 nm upper size bound that defines nanomaterials, as given in definitions by the National Nanotechnology Initiative (NNI) and various other organizations (OECD, EPA, ISO, etc.) (Boverhof et al., 2015). This eliminated zinc from further consideration to determine the need for nano-specific risk (Collier et al., 2015; Martin et al., 2016), as it would not need to be reported as a nanomaterial according to the EPA Section 8a reporting rule (EPA, 2010). Therefore, exposure and hazard of the product related to zinc can be assessed using traditional approaches for bulk zinc metal or release of dissolved ions. Since it was not a nanomaterial, further characterization was not included in this nano-specific study.

SEM analysis confirmed that the light color of the topcoat (both with and without MWCNTs) was due to the inclusion of titanium dioxide (Fig. 2D). TiO_2 is a common white pigment used in many applications, including paints, cosmetics and sunscreens (Weir et al., 2012) which contains particles frequently in the nano-size range (Kaegi, 2008). NIOSH previously published recommended exposure limit (RELs) of $2.4 \text{ mg}/\text{m}^3$ for fine ($> 100 \text{ nm}$) and $0.3 \text{ mg}/\text{m}^3$ for ultrafine (including engineered nanoscale) TiO_2 , as TWA concentrations for up to 10 h/day during a 40-h work week (NIOSH, 2011). The lower ultrafine REL reflects NIOSH's concern for the potential carcinogenicity of ultrafine TiO_2 particles due to increased surface area per unit mass. According to the manufacturer, the TiO_2 pigment was nominally micron-sized, and measurement by SEM (representative images provided in Supplemental Fig. 2) confirmed a mean particle size of 257 nm (Fig. 2D) with upper and lower bounds of 702 nm and 62 nm . While the dominant fraction of TiO_2 observed is above the 100 nm cut off, 3.5% of the 482 particles measured where in $< 100 \text{ nm}$ size range.

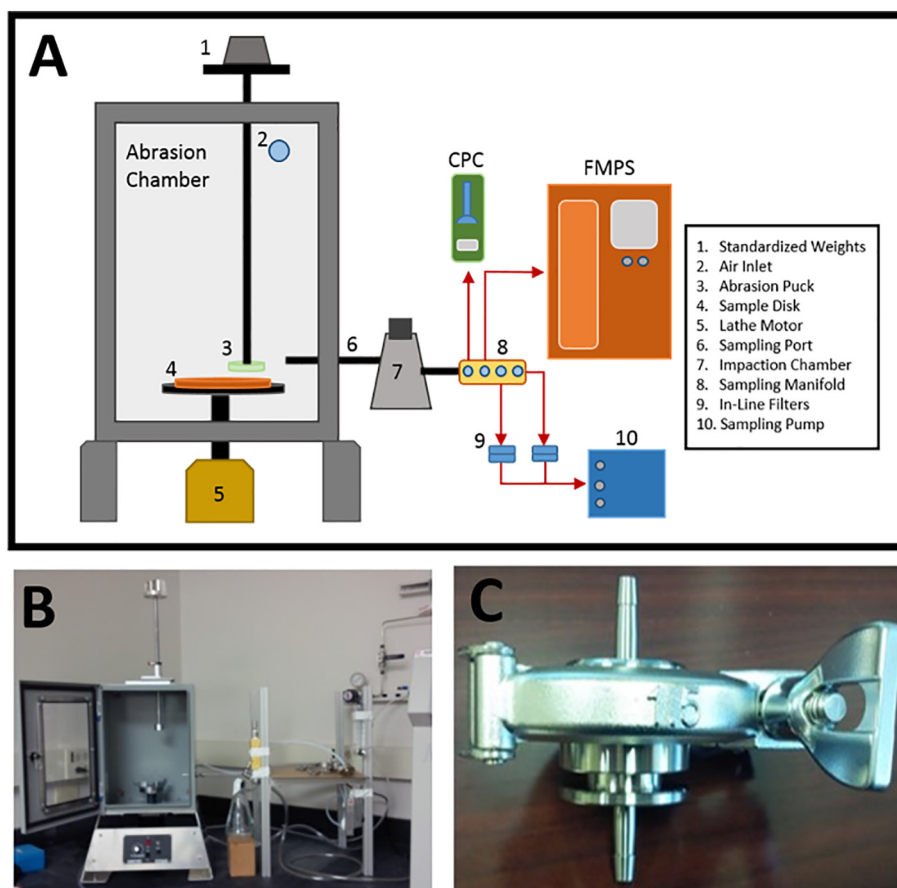


Fig. 1. Diagram of abrasion chamber, including size and flow information (A), image of full system (B) and in-line filter (C).

3.2. Workplace-exposure study

During the two day sampling period, the sampled employees performed a variety of tasks with the personal protective equipment (PPE) as shown in Table 1. Development of batches was performed by employee #1 on both days of sampling. This employee added dry MWCNTs to a wet resin and mixed by hand inside a 5 ft (w) chemical fume hood (Lab Fabricators Co., Cleveland, OH) to produce a small batch in the laboratory. The batch was then dispersed (using a proprietary process) into a primer or coating with the aid of a pneumatic mixer located in the high bay area. This employee was wearing a lab coat, safety glasses, a dust mask, earplugs, and nitrile gloves during this task. Employee #2 was assigned to the office and worked there both days without PPE. Employee #3 split time between the office and high bay production area on both days. When in the high bay area, employee #3 hand painted parts with a CNT-based primer each day. Employee #4 also split time each day between the office and high bay production area. On both days of sampling, employee #4 performed spray coating operations with CNT and non-CNT coatings inside the spray booth. During spray painting, employee #4 wore earplugs, full-body Tyvek, a half-face respirator with organic vapor cartridges, safety glasses, and nitrile gloves.

During application of the paint product, employee exposure to elemental carbon (EC), including MWCNTs, was assessed in relation to the following tasks: development of MWCNT-epoxies and resins and spray coating of CNT-enabled coatings. Over the course of the two days of air sampling, no background-corrected PBZ or area filter-based samples (AS) for EC at the respirable size fraction were found to have concentrations above the NIOSH REL of $1 \mu\text{g}/\text{m}^3$ (Table 1). The background-corrected inhalable fraction was also below $1 \mu\text{g}/\text{m}^3$ in all cases except for the PBZ of spray-booth operator ($12.31\text{--}14.94 \mu\text{g}/\text{m}^3$) and on

employee #3 who worked in the high bay area ($1.52\text{--}2.29 \mu\text{g}/\text{m}^3$). The task-based area samples (inside the spray booth) had the highest inhalable EC concentrations ($0.99 \mu\text{g}/\text{m}^3$).

We found that the PBZ samples collected for employee #4 who worked in the spray booth and high bay areas showed higher inhalable EC concentrations than did the area samples collected in the spray booth. There are several possible reasons for this apparent discrepancy: 1) this worker directly handled gram quantities of raw MWCNT for an hour each day and also worked on dispersing the MWCNTs into the paint product. This could result in higher concentrations of EC exposure than spray booth operations; and 2) PBZ concentrations in the spray booth might have been higher than AS concentrations, due to the measurements being collected closer to the exposure source for the PBZ than the area samples. This pattern has been observed previously in studies of CNT-exposed workers (Dahm et al., 2012).

While CNTs are a subset of the measured EC, the carbon measurement may also include soot or organic carbon from the polymer matrix. The fractions for soot and MWCNTs in the total EC concentrations measured here are unknown. TEM analysis confirmed the presence of MWCNTs, and other particulates, in seven different area or task-based samples throughout both days of sampling (Fig. 3). These analyses showed exposed MWCNTs, however the particles were often agglomerated with other MWCNTs or other material and no free MWCNTs were observed. TEM image analysis showed MWCNT-containing structures were most commonly found within material ranging in size from 5 to $10 \mu\text{m}$, followed by $2\text{--}5 \mu\text{m}$ and $> 10 \mu\text{m}$. A concentration measurement was made by counting all MWCNT-containing structures (with no bias to size or shape) as a function of the air volume passed through the filter. For the PBZ of the spray booth operator, the filters were overloaded with material and a quantitative measurement of MWCNT structures could not be obtained. In all other PBZ and AS, the

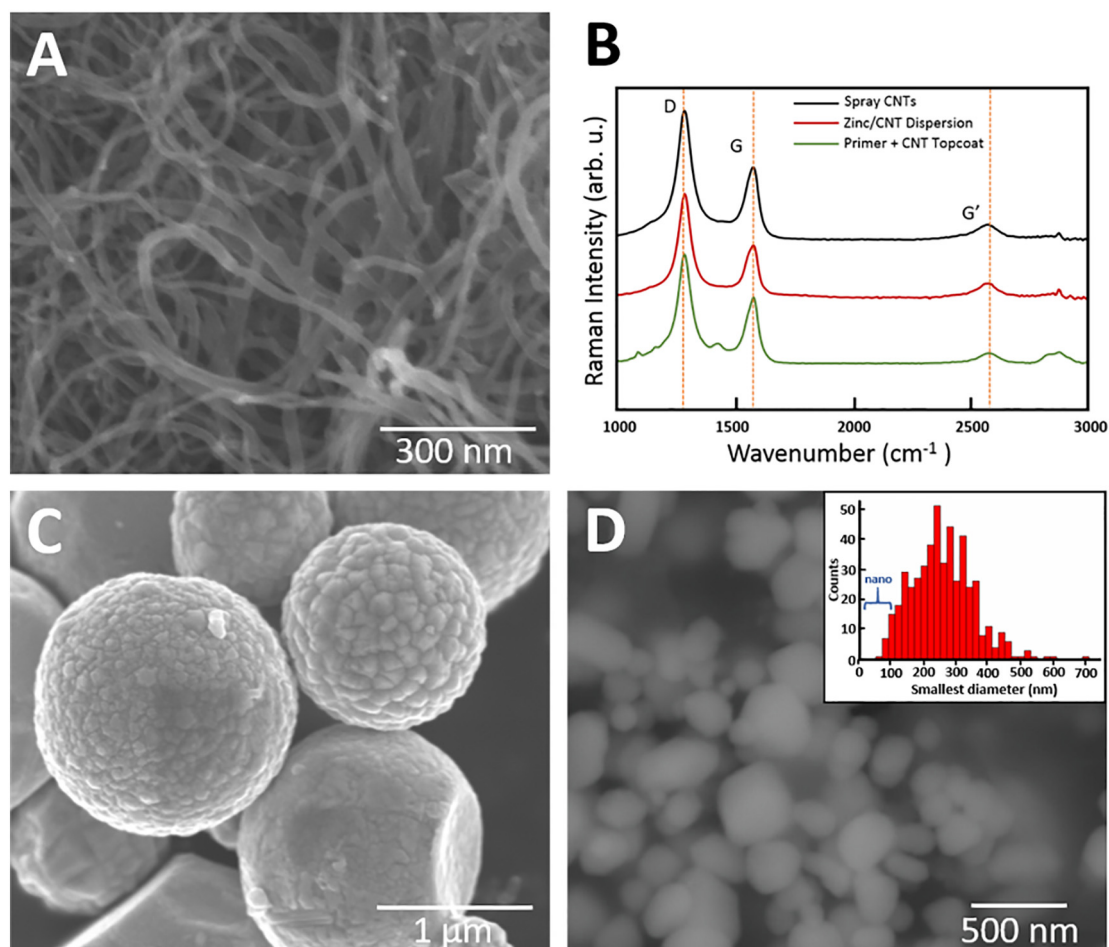


Fig. 2. SEM images of carbon nanotubes included in the anticorrosive coating provided by Tesla (A), Raman spectra showing characteristic CNT peaks dispersed in the raw, unmixed powder and in the coated Tesla materials, compared to a control of pure CNTs (B), SEM images of zinc particles in the raw powder (C), TiO₂ particles (D) observed on the surface of the primer and topcoat, and the particle size distribution as measured across the smallest diameter.

MWCNT-containing structures did not exceed a concentration of 0.02 structures/cm³. The lack of respirable size MWCNT structures does come with an important caveat: agglomerated structures may dissociate once inside the lungs, potentially making larger than respirable size fractions (e.g. thoracic and inhalable) relevant to health effects. Although a reference or benchmark level of 0.01 fibers/cm³ for MWCNT has been established in the UK, Germany and Switzerland (Ellenbecker et al., 2018), this is acknowledged to be based on analogy to asbestos rather than direct evidence of risk, highlighting the need to better-characterize this aspect of exposure.

3.3. Chamber-based release testing

Aerosolized particle size distributions collected during abrasion of un-weathered material by FMPS showed differences in the aerosolized particles released from the various samples, with the assumption that all particles released were spherical. Samples containing TiO₂-pigmented topcoats (primer with MWCNT-topcoat and primer with non-MWCNT-topcoat) released aerosolized particles primarily in the nanorange (< 100 nm), while those without TiO₂ (bare steel and primer only controls) had mean particle size distributions centered between 110 and 140 nm (Fig. 4). Weathering via UV exposure prior to abrasion of the MWCNT and non-MWCNT topcoat samples did not shift the median particle size of ~40 nm, however there significant changes to both ends of the particle size distribution tails. Before UV treatment, particle distribution of the topcoat samples appears bimodal, with the non-MWCNT topcoat in particular having a significant second peak

around 220 nm. UV-treatment reduces the broadness of the large-particle size tail, as well as adopts a more unimodal distribution. The primer only (no topcoat) shows unimodal distributions before and after weathering, as well as a noticeable shift in median size distribution from 124 nm to 107 nm. For the lower bounds of the distribution, a small peak around 10 nm appears in all UV-weathered specimens.

Fig. 5A shows representative SEM image from the filters used to collect particles released during abrasion of a weathered sample with both the MWCNT primer and MWCNT/TiO₂ topcoat. The image shows multiple TiO₂ particles surrounding a comparatively large (4 μm) zinc particle. The EDS scans for titanium (Fig. 5C) co-located with oxygen (Fig. 5D) confirm the small particles as TiO₂. Release of nano-sized particles during abrasion is typical of many materials (Kingston et al., 2014), and in this case included nanoparticles released from the TiO₂ pigment.

4. Discussion

Carbon nanotubes may be released from a composite in one of four ways: completely embedded within the matrix, partially embedded in the matrix, completely released from the matrix as individual or fragmented CNTs, or as agglomerated CNT structures. The ultimate hazard of freely released CNTs remains uncertain, as one study found potential carcinogenicity of high aspect ratio (i.e., long and narrow) CNTs, synonymous to asbestos-related concerns (Poland et al., 2008; Chernova et al., 2017), while another study found no effects from injected MWCNTs in mice (Takanashi et al., 2012). In addition, other studies

Table 1
Workplace-exposure elemental carbon (EC) measurements.

| Type of sample ^a | EC fraction | Job duty/process | Engineering controls/PPE used | 8-h TWA EC ($\mu\text{g}/\text{m}^3$) (Bkg corr) | |
|-----------------------------|-------------|--|---|--|---------------------------|
| | | | | Day 1 | Day 2 |
| PBZ | Respirable | Employee #1 (Lab area) | MWCNT weigh out and mixing production/conducted inside chemical fume hood. Dispersion in high bay area/room exhaust ventilation, lab coat, safety glasses, dust mask, nitrile gloves | ND ^b | 0.10 |
| | Inhalable | | | 0.90 | 0.71 |
| PBZ | Respirable | Employee # 2 (Office area) | Worked in the office/no PPE | ND ^b | < Background ^c |
| PBZ | Inhalable | Employee #3 (High bay area) | Hand painted parts with CNT-based primer/room exhaust ventilation, lab coat, safety glasses, nitrile gloves | 0.57 | 0.45 |
| | Respirable | | | ND ^b | 0.05 |
| PBZ | Respirable | Employee #4 (Spray booth/high bay area) | Sprayed CNT paint formulation/conducted in spray paint booth, with safety glasses, Tyvek coveralls, 1/2 face respirator with organic vapor cartridges, nitrile gloves | 1.52 | 2.29 |
| | Inhalable | | | 0.21 | < Background ^c |
| AS | Respirable | High bay area (Spraying operations) | | 14.94 | 12.31 |
| | Inhalable | | | ND ^b | 0.20 |
| AS | Respirable | Lab area (CNT batch development) | | 0.27 | 0.42 |
| | Inhalable | | | ND ^b | < Background ^c |
| AS | Respirable | Inside spray booth (Before spraying) | | 0.00 | < Background ^c |
| AS | Inhalable | Inside spray booth (During spraying CNTs) | | ND ^b | ND ^b |
| | Respirable | | | ND ^b | ND ^b |
| AS | Inhalable | Inside spray booth (During spraying non-CNTs) | | < Background ^c | ND ^b |
| | Respirable | | | ND ^b | ND ^b |
| | | | | 0.99 | ND ^b |

Numbers in bold are samples that were found to be above the NIOSH REL of $1 \mu\text{g}/\text{m}^3$.

^a PBZ: personal breathing zone; AS: area sample.

^b ND-not detectable. The limit of detection (LOD) for the 25-mm filters was $0.4 \mu\text{g}$ EC/filter.

^c The background concentrations for respirable EC was $0.10 \mu\text{g}/\text{m}^3$ and $0.55 \mu\text{g}/\text{m}^3$ for days 1 and 2, respectively. The background concentrations for inhalable EC were $0.57 \mu\text{g}/\text{m}^3$ and $0.76 \mu\text{g}/\text{m}^3$ for days 1 and 2, respectively.

have found short MWCNT fragments (< 300 nm) are associated with acute phase response, pulmonary inflammation and fibrosis (Poulsen et al., 2015, 2016, 2017). Bishop et al. (2017) found that toxicity of CNT-containing composite particulates produced by sanding was inconsistently elevated, compared to neat composite, which may be related to smaller particulate size in the CNT-containing composite. It should also be addressed that several limitations are present in the current body of work regarding CNT inhalation exposure including a lack of consistency in the composition of CNTs evaluated at various step in the carcinogenic pathway, limitations in animal studies, and the absence of the human studies (Kobayashi et al., 2017; Pauluhn, 2010). Most evaluations of CNTs also have focused on the health effects of MWCNT-7 and it is unknown if data can be applied to other forms of MWCNTs and SWCNTs (Kuempel et al., 2017; Kobayashi et al., 2017; Fukushima et al., 2018).

Until definitive hazard information is available, it is important as a precautionary approach to determine whether individual CNTs of any form are released from the coating matrix, to define exposure potential for human and environmental receptors (Harper et al., 2015; Schlagenhauf et al., 2015), and thus the potential for risk concern. However, detecting individually released CNTs, especially in a complex matrix (Doudrick et al., 2012) is difficult and labor intensive, especially in context of proving an absence or negligible quantity of CNTs for exposure assessments (Koivisto et al., 2018). Raman spectroscopy, among other methods (Doudrick et al., 2013), can confirm the presence of carbon nanotubes, but cannot identify whether the CNTs are freely released or partially/completely embedded in the coating matrix. Previously published studies of MWCNTs embedded in different matrices also did not find release of free MWCNTs following robust analysis (Petersen et al., 2014; EPA, 2013). However, this does not exclude the potential for free MWCNTs to be present, and this should be recognized accordingly in EHS assessments.

SEM and Raman analysis of the material released from the TESLA anti-corrosive coatings via abrasion confirms the presence of embedded

MWCNTs both on the filters and in the released powder collected from the abrasion chamber (Fig. 6). Despite extensive SEM analysis and previous confirmation that the filter system can trap free MWCNTs, we were unable to identify any individually-released MWCNTs from any sample analyzed during this testing (see Supplemental Figs. S3–S6). UV weathering prior to abrasion significantly increased the number of MWCNTs protruding from the matrix, as identified in SEM analysis, but again did not produce any identifiable, individually released MWCNTs. It is difficult to make a definitive statement that individual MWCNTs are not released; a study by Koivisto et al. (2018) determined that proper assessment of individually released nanofibers with an acceptable error level at a concentration of $1 \text{ fiber}/\text{cm}^3$ would require an unfeasible assessment of 4×10^4 images. Absence of discoverable MWCNTs by this technique does not provide concrete evidence of their absence, and future studies using this system should utilize NIOSH fiber counting rules (Ashley and O'Connor, 2016; NIOSH, 1994a, 1994b). Additionally, until improved sampling and analytical methods are developed, further work is needed to determine an acceptable framework for selecting multiple MWCNT detection methods to provide multiple lines of evidence for the presence or absence of MWCNTs (Alberts et al., 2018).

Analysis of the size distribution obtained by the FMPS suggests weathering influences the release of nano-size material from the coating. As with many particle sizing instrumentation, FMPS is unbiased towards elemental composition, making it challenging to identify what the measured nano-sized particles are. However, it can be noted that the small normalized fraction of particles that appears around 10 nm is not dependent on whether the topcoat contains CNTs and is also observed in the primer. All three of these samples contain TiO_2 , which suggests that UV weathering enables release of nano-size TiO_2 from the coating, if these nano-size particles are not simply nano-size fragments of the matrix material itself. This also corresponds with the lack of free CNTs found on the SEM filters. The increase of nano-size material during weathering is likely due to degradation of the polymer

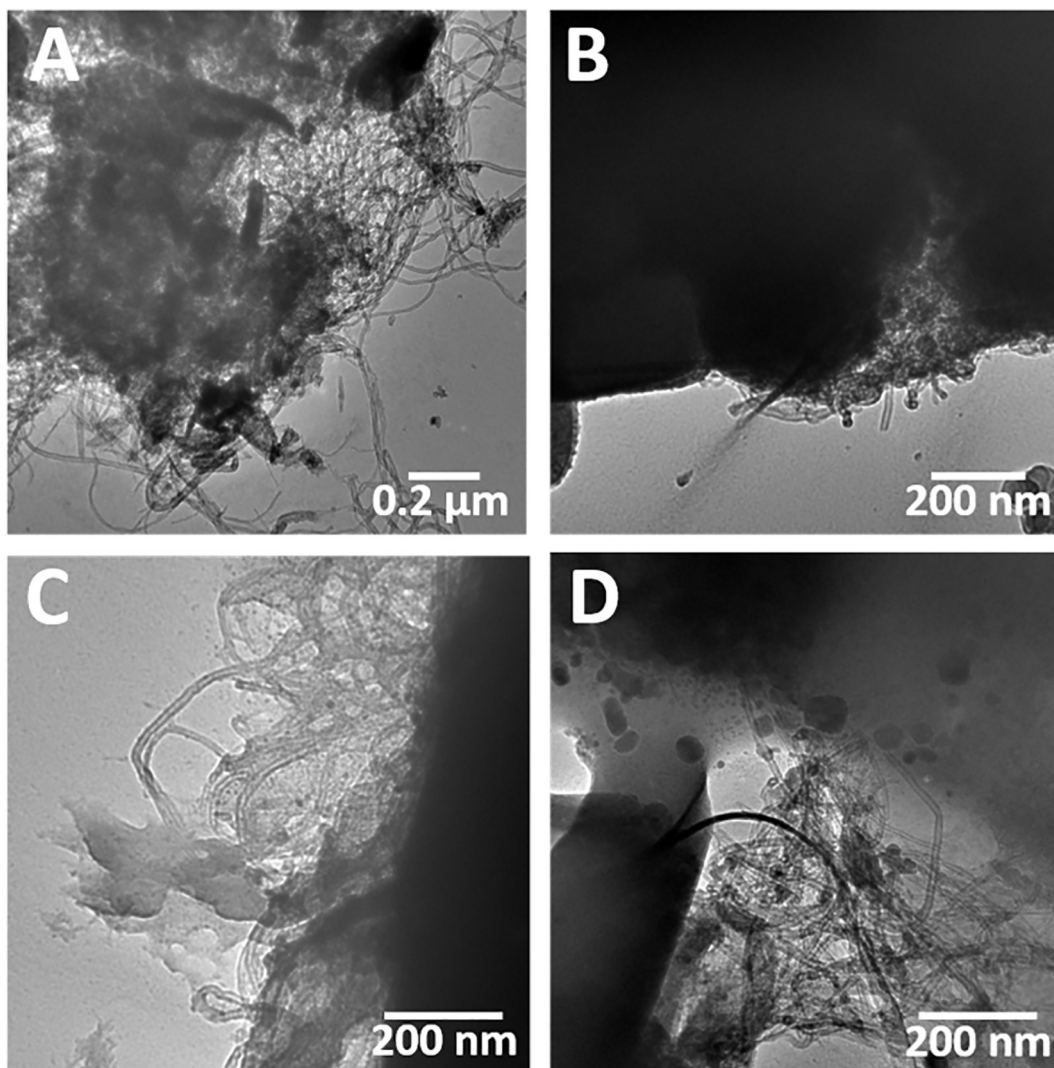


Fig. 3. TEM images showing typical CNT-containing structures identified in personal breathing zone (PBZ) and area samples (AS) for (A) PBZ employee #3 (high bay area), (B) PBZ employee #4 (spray booth/high bay area), (C) AS inside spray booth, (D) AS inside blasting cabinet.

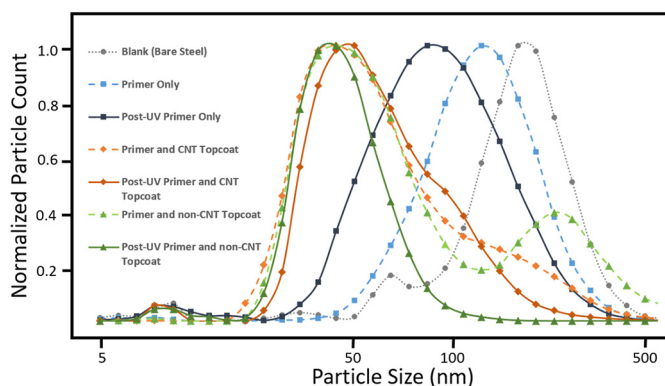


Fig. 4. Normalized particle size distribution data for abrasion of coated samples with and without UV weathering. The majority of particles released by samples with TiO₂-containing topcoats (white and light gray) were in the nanorange (< 100 nm), while those without TiO₂ pigmentation were primarily larger than 100 nm.

matrix due to UV-exposure. The loss of the broad tail in the size distribution above 100 nm in the weathered topcoat samples may also be a result of the matrix material breaking down into smaller fragments

during abrasion as a result of UV degradation. It should be noted that the FMPS is prone to artifacts which can make interpretation of size distribution challenging, as it tends to underestimate the size of particle in the > 200 nm size bins, as well having an inherent tri-modal size distribution at 10.7, 19.1, and 29.4 nm size bins (Levin et al., 2015; Zimmerman et al., 2015). While these artifacts do not greatly influence the overall trends we observe here it may be advisable in future studies to cross-check these measurements with and scanning mobility particle sizer (SMPS) (Jeong and Evans, 2009).

In the case of the anti-corrosive coating material studied here, characterization studies determined a lack of nano-specific hazard due to zinc, and after thorough analysis, a lack of evidence for individually released MWCNTs. There was also evidence for a 3% fraction of nano-TiO₂ in the pigment and a potential release of nano-TiO₂ following abrasion testing. While the median size of the TiO₂ pigment would exclude it from consideration as a nanoparticle, the trace amount of nano-size particles in the tail end of the size distribution (Fig. 2D) calls into question if TiO₂ should still be considered a nanomaterial in this case for risk assessment. TiO₂ tested in ambient laboratory conditions may be considered to have relatively low hazard compared to other nano-metals, although the crystalline form of released TiO₂ may be relevant as the toxicity of the anatase form in presence of continuous sunlight increases its toxicity by > 2 orders of magnitude (Ma et al., 2014; Bar-Ilan et al., 2013; Diamond et al., 2017). A study by Gerloff

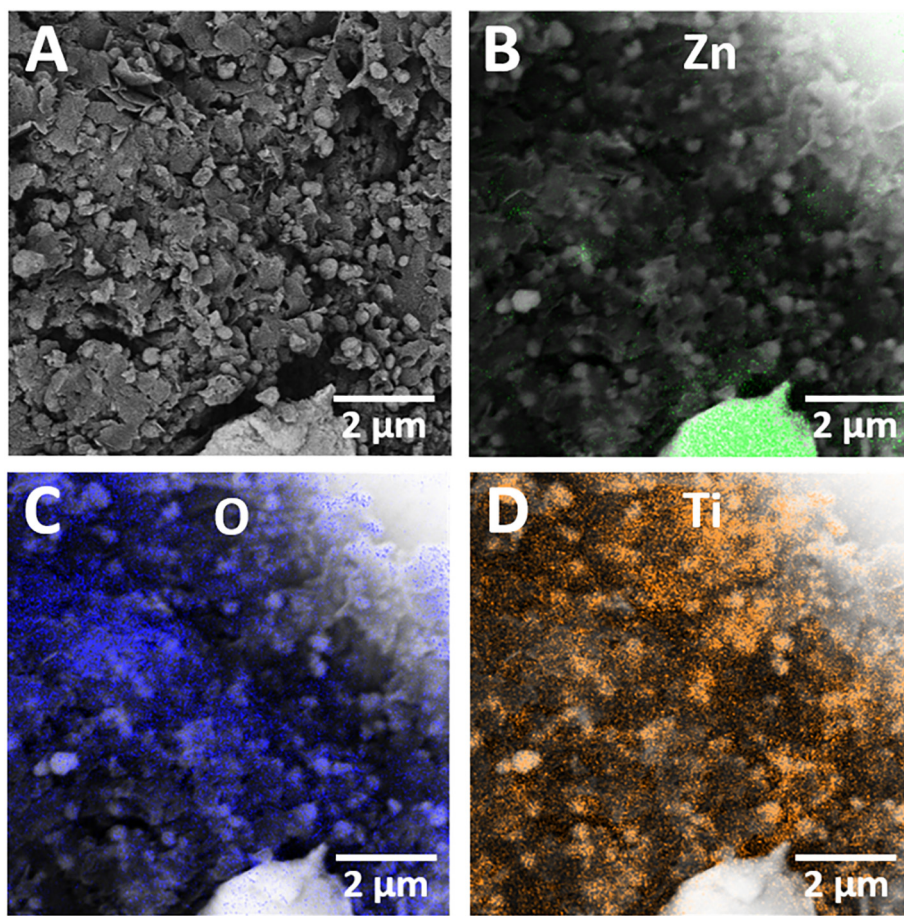


Fig. 5. SEM image (A) of particles collected from the chamber during abrasion of a sample coated with primer and CNT/TiO₂ topcoat. Panels B–D show EDS color images representing the presence of zinc (B), titanium (C) and oxygen (D, co-located with Ti for TiO₂). (For interpretation of the references to color in this figure legend, the reader is referred to the web version of this article.)

et al. (2012) showed anatase/rutile compositions of TiO₂ exhibited higher toxicity per unit surface area in human colon cells than pure anatase. However, the anatase form of TiO₂ can induce oxidative stress in combination with UV light, with a LC50 value of 0.03 mg/L (Wang et al., 2014), a hazard category of “highly toxic”. In addition, Warheit et al. (2007) demonstrated increased pulmonary toxicity of 80/20 anatase/rutile TiO₂ versus pure rutile in rats via intratracheal administration.

The EPA reporting rule states that any substance that consists of > 1% by mass of ENMs should be considered a nanomaterial, however there is debate whether particle number is a more relevant metric when evaluating pulmonary inflammatory response due to ENM exposure (Wittmaack, 2007). While several organizations including the European Commission (EC), the Swiss Federal Office of Public Health (FOPH), and Norwegian Environmental Agency (NEA) recommends that a material be classified as “nano” when 50% a material by particle number is below the 100 nm threshold, the Australian Government Department of Health and Ageing place the threshold as low as 10% (Boverhof et al., 2015). The EC also suggests that composition as low as 1% by particle number could be considered in some cases. Furthermore, other agencies such as the International Organization for Standardization (ISO), Taiwan Council of Labor Affairs (CLA) and Health Canada have no stated distribution thresholds for mass or particle counts. Other inconsistencies between these organizations include whether agglomeration is considered, solubility of the ENM and if it was intentionally manufactured or engineered (Boverhof et al., 2015), taken together this raises the question for how borderline ENM materials should be handled in regards to health and hazard assessments.

From the FMPS and SEM evaluations, TiO₂ represents a case where there may be enough uncertainty to justify its inclusion with the CNTs for evaluation and testing as a precautionary measure. It should also be

considered that the relative proportion of the size distribution tail in the nanorange may increase after inhalation, as inhaled TiO₂ can travel to the gastrointestinal via the mucociliary clearance pathway where it can be subject to digestive processes (Gerloff et al., 2012). TiO₂ was not taken into consideration for the workplace exposure assessment, highlighting the need for a rigorous method for characterization of advanced materials to ensure all potentially released hazardous ENMs are identified and evaluated. Since it was not the active ingredient used in the application for a nano-specific and unique property, it is unclear if it requires reporting as part of the EPA reporting rule.

This study provides a demonstration to estimate exposure to inform EHS risk decisions for a MWCNT-enabled anti-corrosion coating. This material may provide environmental benefit by using MWCNTs to reduce zinc loading in coating applications, but use of MWCNTs during application and mechanical removal brings unique EHS questions. The workplace exposure study provided evidence for overall low exposures, with all respirable (d₅₀ = 4 μm) samples being below the NIOSH REL for CNTs. In a large study of CNT-exposed workers using the same measurement methods employed here, the arithmetic mean inhalable PBZ EC and TEM structure count concentrations were 6.47 μg/m³ and 0.084 structures/cm³, respectively (Dahm et al., 2015). Only the spray booth operation exceeded one or both of these mean values. The highest potential for exposure was found during formulation and spraying of CNT coatings. However, the use of local exhaust ventilation and enclosures reduce the risk of worker exposure and migration of nanomaterials outside of the production areas. Further mitigation of exposure can be accomplished with the addition of powered air purifying respirators (Koivisto et al., 2015).

While NIOSH recommends an elemental carbon REL based on mass concentration, there is some debate over whether number concentration is a more appropriate metric, especially in regards to CNTs. The

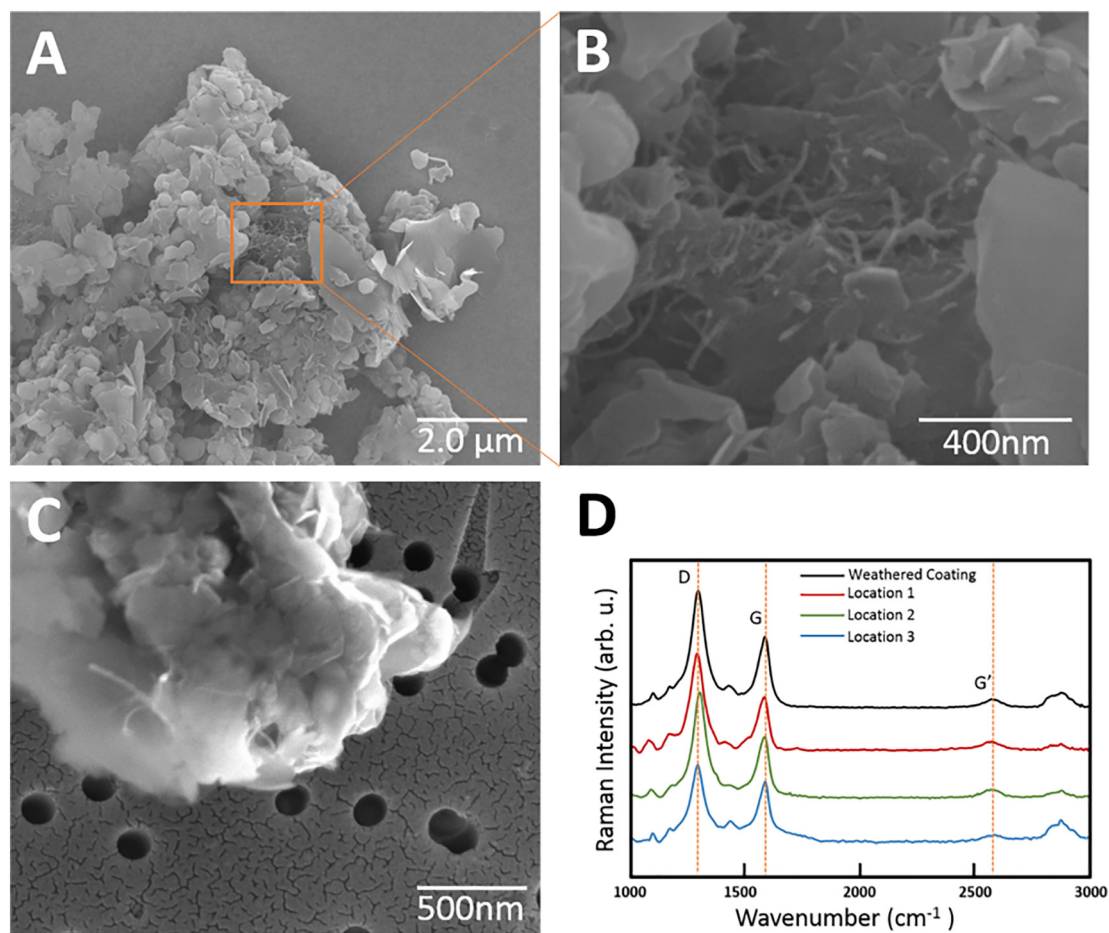


Fig. 6. SEM images (A, B and C) showing exposed CNTs after abrasion of UV-weathered samples (primer + CNT topcoat). Panel D shows Raman spectra confirming the presence of CNTs on the SEM filter (locations 1–3) and comparison to the weathered CNT coating.

British Standard Institute (BSI), Swiss Accident Insurance Funds (SUVA), and the German Institute for Occupational Safety and Health (IFA) recommend a number based REL for CNTs and asbestos fibers of 0.01 f/cm^3 (BSI, 2007; SUVA, 2018; van Broekhuizen and Dorbeck-Jung, 2013). The Japanese National Institute of Advanced Industrial Science and Technology (AIST) has proposed mass based RELs of $30 \mu\text{g/m}^3$ for SWCNTs and $80 \mu\text{g/m}^3$ for MWCNTs (NEDO, 2011). Concerns with the mass based approach to RELs include the health effects of CNTs correlating with number inhaled instead of total mass, as $1 \mu\text{g/m}^3$ of CNTs could be equivalent to anywhere between 0.01 f/cm^3 and $300,000 \text{ f/cm}^3$ based on the size of the fiber (Ellenbecker et al., 2018). Additionally, current analytical methods lack the ability to distinguish CNT mass from other carbon sources collected on air filters. While number metrics may be a more appropriate assessment, CNT agglomeration can alter toxicity (Wick et al., 2007) and CNTs can only be observed by electron microscopy, unlike asbestos fibers, making number-based assessments prohibitively more costly.

Based on the lack of evidence for free CNTs, this product may potentially pass requirements for exposure. However, knowledge is limited on how inhalation of embedded/exposed CNTs could affect human health, and some studies have suggested matrix material is a driving factor in toxicity (Wohlleben et al., 2011; Smulders et al., 2014; Saber et al., 2012). Characterization of the coating found that TiO_2 , used as a pigment in the coating and not anticipated as a candidate for nano-specific scrutiny, contained a fraction of nano-sized particles, raising the question if additional attention should be required (Brame et al., 2015). UV-weathering and abrasion experiments simulating intended use during the lifetime and end of use and removal emphasize the importance of implementing an organized approach to assess EHS

implications of products containing ENMs. This work helps to further understanding of risk and exposure assessments, including robust CNT characterization by multiple methods. While this work is primarily focused on product development, product application and intended use, consideration to a full life-cycle based approach for this material, including end-of-life removal via sandblasting, is an additional necessary component to be explored in future studies.

Disclaimers

The findings and conclusions of this report are those of the authors and do not necessarily reflect those of the National Institute for Occupational Safety and Health. Mention of trade names does not imply endorsement by the U.S. Government.

Acknowledgements

This work was funded by the US Army Environmental Quality/Installations (EQ/I) research program. The core study was funded by the Environmental Consequences of Nanotechnology focus area (Army 6.2–6.3). The views and opinions expressed in this paper are those of the individual authors and not those of the U.S. Army, or other sponsor organizations. The authors also thank the National Institute for Occupational Safety and Health (NIOSH) Nanotechnology Research Center for partial funding of this work.

Appendix A. Supplementary data

Supplementary data to this article can be found online at <https://>

doi.org/10.1016/j.impact.2018.10.002.

References

- Alberts, E., et al., 2018. Methodological studies for quantifying airborne release of nano- and nano-enabled materials using a fast mobility particle sizer. *NanoImpact* 11, 92–98.
- Ashley, K., O'Connor, P.F., 2016. *NIOSH Manual of Analytical Methods (NMAM)*, 5th ed. Available online: <http://www.cdc.gov/niosh/nmam>.
- Bar-Ilan, O., et al., 2013. TiO₂ nanoparticle exposure and illumination during zebrafish development: mortality at parts per billion concentrations. *Environ. Sci. Technol.* 47, 4726–4733.
- Birch, M.E., et al., 2011a. Exposure and emissions monitoring during carbon nanofiber production—part I: elemental carbon and iron-soot aerosols. *Ann. Occup. Hyg.* 55 (9), 1016–1036.
- Birch, M.E., et al., 2011b. Exposure and emissions monitoring during carbon nanofiber production—part II: polycyclic aromatic hydrocarbons. *Ann. Occup. Hyg.* 55 (9), 1037–1047.
- Bishop, L., et al., 2017. In-vivo toxicity assessment of occupational components of the carbon nanotube life cycle to provide context to potential health effects. *ACS Nano*. <https://doi.org/10.1021/acsnano.7b03038>.
- Bokobza, L., et al., 2015. Raman spectra of carbon-based materials (from graphite to carbon black) and of some silicone composites. *C 1* (1), 77.
- Boverhof, D., et al., 2015. Comparative assessment of nanomaterial definitions and safety evaluation considerations. *Regul. Toxicol. Pharmacol.* 73, 137–150.
- Brame, J.A., et al., 2015. EHS testing of products containing nanomaterials: what is nanorelease? *Environ. Sci. Technol.* 49 (19), 11245–11246.
- van Broekhuizen, P., Dorbeck-Jung, B., 2013. Exposure limit values for nanomaterials—capacity and willingness of users to apply a precautionary approach. *J. Occup. Environ. Hyg.* 10 (1), 46–53.
- BSI, 2007. *Nanotechnologies—part 2: guide to safe handling and disposal of manufactured nanomaterials*. In: British Standards Institute. Report No. 978 0580 60,832 2.
- Chernova, T., et al., 2017. Long-fiber carbon nanotubes replicate asbestos-induced mesothelioma with disruption of the tumor suppressor gene *Cdkn2a (Ink4a/Arf)*. *Curr. Biol.* 27 (21), 3302–3314.
- Collier, Z., et al., 2015. Tiered guidance for risk-informed environmental health and safety testing of nanotechnologies. *J. Nanopart. Res.* 17 (3), 1–21.
- Dahm, M.M., et al., 2012. Occupational exposure assessment in carbon nanotube and nanofiber primary and secondary manufacturers. *Ann. Occup. Hyg.* 56 (5), 542–556.
- Dahm, M.M., et al., 2015. Carbon nanotube and nanofiber exposure assessments: an analysis of 14 site visits. *Ann. Occup. Hyg.* 59 (6), 705–723.
- Diamond, S.A., et al., 2017. Assessment of the potential hazard of nano-scale TiO₂ in photocatalytic cement: application of a tiered assessment framework. *NanoImpact* 8, 11–19.
- Doudrick, K., et al., 2012. Detection of carbon nanotubes in environmental matrices using programmed thermal analysis. *Environ. Sci. Technol.* 46 (22), 12246–12253.
- Doudrick, K., et al., 2013. Extraction and quantification of carbon nanotubes in biological matrices with application to rat lung tissue. *ACS Nano* 7 (10), 8849–8856.
- Ellenbecker, M., et al., 2018. The difficulties in establishing an occupational exposure limit for carbon nanotubes. *J. Nanopart. Res.* 20, 131.
- EPA, 2010. *Control of nanoscale materials under the toxic substances control act*. <http://www.epa.gov/oppt/nano/#existingmaterials>.
- EPA, 2013. *Comprehensive Environmental Assessment Applied to Multiwalled Carbon Nanotube Flame-retardant Coatings in Upholstery Textiles: A Case Study Presenting Priority Research Gaps for Future Risk Assessments (Final Report)*.
- Evans, D.E., et al., 2015. Aerosol monitoring during carbon nanofiber production: mobile direct-reading sampling. *Ann. Occup. Hyg.* 54 (5), 514–531.
- Froggett, S.J., et al., 2014. A review and perspective of existing research on the release of nanomaterials from solid nanocomposites. *Part. Fibre Toxicol.* 11, 17.
- Fukushima, S., et al., 2018. Carcinogenicity of multi-walled carbon nanotubes: challenging issue on hazard assessment. *J. Occup. Health* 60, 10–30.
- Gerloff, K., et al., 2012. Distinctive toxicity of TiO₂ rutile/anatase mixed phase nanoparticles on caco-2 cells. *Chem. Res. Toxicol.* 25 (3), 646–655.
- Gohler, D., et al., 2013. Nanoparticle release from nanocomposites due to mechanical treatment at two stages of the lifecycle. *J. Phys. Conf. Ser.* 429, 012045.
- Harper, S., et al., 2015. Measuring nanomaterial release from carbon nanotube composites: review of the state of the science. *J. Phys. Conf. Ser.* 617, 012026.
- Hirth, S., et al., 2013. Scenarios and methods that induce protruding or released CNTs after degradation of nanocomposite materials. *J. Nanopart. Res.* 15, 1–15.
- Huang, G., et al., 2012. Evaluation of airborne particle emissions from commercial products containing carbon nanotubes. *J. Nanopart. Res.* 14. <https://doi.org/10.1007/s11051-012-1231-830>.
- IARC, 2017. *IARC monographs on the evaluation of carcinogenic risks to humans, volume 111. In: Some Nanomaterials and Some Fibers*, Lyon, France: Available from: <https://monographs.iarc.fr/wp-content/uploads/2018/06/mono111.pdf>.
- Jeong, C.H., Evans, G., 2009. Inter-comparison of a fast mobility particle sizer and a scanning mobility particle sizer incorporating an ultrafine water-based condensation particle counter. *Aerosol Sci. Technol.* 43 (4), 364–373.
- Kaegi, R., 2008. Synthetic TiO₂ nanoparticle emission from exterior facades into the aquatic environment. *Environ. Pollut.* 156 (2), 233–239.
- Kaiser, D., et al., 2014. *Methods for the Measurement of Release of MWCNTs From MWCNT-polymer Composites*. White Paper. National Institute of Standards and Technology, Gaithersburg, MD.
- Kingston, C., et al., 2014. Release characteristics of selected carbon nanotube polymer composites. *Carbon* 68, 33–57.
- Kobayashi, et al., 2017. Review of toxicity studies of carbon nanotubes. *J. Occup. Health* 59, 394–407.
- Koivisto, A.J., et al., 2015. Workplace performance of a loose-fitting powered air purifying respirator during nanoparticle synthesis. *J. Nanopart. Res.* 17, 177.
- Koivisto, A.J., et al., 2017. Quantitative material releases from products and articles containing manufactured nanomaterials: towards a release library. *Nano* 5, 119–132.
- Koivisto, A.J., et al., 2018. Occupational exposure during handling and loading of halloysite nanotubes – a case study of counting nanofibers. *NanoImpact* 10, 153–160.
- Kuempel, E.D., et al., 2017. Evaluating the mechanistic evidence and key data gaps in assessing the potential carcinogenicity of carbon nanotubes and nanofibers in humans. *Crit. Rev. Toxicol.* 47, 1–58.
- Lehman, J.H., et al., 2011. Evaluating the characteristics of multiwall carbon nanotubes. *Carbon* 49 (8), 2581–2602.
- Levin, M., et al., 2015. Limitations in the use of unipolar charging for electrical mobility sizing instruments: a study of the fast mobility particle sizer. *Aerosol Sci. Technol.* 49 (8), 556–565.
- Ma, H., et al., 2014. Impact of solar UV radiation on toxicity of ZnO nanoparticles through photocatalytic reactive oxygen species (ROS) generation and photo-induced dissolution. *Environ. Pollut.* 193, 165–172.
- Martin, D.P., et al., 2016. Nanosilver conductive ink: a case study for evaluating the potential risk of nanotechnology under hypothetical use scenarios. *Chemosphere* 162, 222–227.
- Møller, P., Jacobsen, N.R., 2017. Weight of evidence analysis for assessing the genotoxic potential of carbon nanotubes. *Crit. Rev. Toxicol.* 47, 867–884.
- National Institute for Occupational Safety and Health (NIOSH), 2011. *Occupational Exposure to Titanium Dioxide: Current Intelligence Bulletin 63*. Department of Health and Human Services, (NIOSH) Publication No. 2011–160. <https://www.cdc.gov/niosh/docs/2011-160/pdfs/2011-160.pdf> (April).
- NEDO, 2011. *Risk Assessment of Manufactured Nanomaterials: Carbon Nanotubes (CNTs)*. New Energy and Industrial Technology Development Organization.
- NIOSH, 1994a. Method for determination of asbestos in air using positive phase contrast microscopy. In: *NIOSH Method 7400*. National Institute for Occupational Safety and Health First Issued: 1985, Cincinnati, OH (Current revision).
- NIOSH, 1994b. Method for determination of asbestos in air using transmission electron microscopy. In: *NIOSH Method 7402*. National Institute for Occupational Safety and Health 1986, Cincinnati, OH (Current revision).
- Analysis of carbon nanotubes and nanofibers on mixed cellulose ester filters by transmission electron microscopy: chapter CN. By Birch ME et al. In: NIOSH, Ashley, K., O'Connor, P.F. (Eds.), *NIOSH Manual of Analytical Methods*, 5th ed. U.S. Department of Health and Human Services, Centers for Disease Control and Prevention, National Institute for Occupational Safety and Health, DHHS (NIOSH) Publication No. 2014–151, Cincinnati, OH. <https://www.cdc.gov/niosh/nmam/pdf/chapter-cn.pdf>.
- Nowack, B., et al., 2013. Potential release scenarios for carbon nanotubes used in composites. *Environ. Int.* 59, 1–11.
- Pauluhn, J., 2010. Subchronic 13-week inhalation exposure of rats to multiwalled carbon nanotubes: toxic effects are determined by density of agglomerate structures, not fibrillar structures. *Toxicol. Sci.* 113, 226–242.
- Petersen, E.J., et al., 2011. Potential release pathways, environmental fate, and ecological risks of carbon nanotubes. *Environ. Sci. Technol.* 45 (23), 9837–9856.
- Petersen, E.J., et al., 2014. Methods to assess the impact of UV irradiation on the surface chemistry and structure of multiwall carbon nanotube epoxy nanocomposites. *Carbon* 69, 194–205.
- Petersen, E.J., et al., 2015. Adapting OECD aquatic toxicity tests for use with manufactured nanomaterials: key issues and consensus recommendations. *Environ. Sci. Technol.* 49 (16), 9532–9547.
- Poland, C.A., et al., 2008. Carbon nanotubes introduced into the abdominal cavity of mice show asbestos-like pathogenicity in a pilot study. *Nat. Nanotechnol.* 3 (7), 423–428.
- Poulsen, S.S., et al., 2015. MWCNTs of different physicochemical properties cause similar inflammatory responses, but differences in transcriptional and histological markers of fibrosis in mouse lungs. *Toxicol. Appl. Pharmacol.* 284, 16–32.
- Poulsen, S.S., et al., 2016. Multi-walled carbon nanotube physicochemical properties predict pulmonary inflammation and genotoxicity. *Nanotoxicology* 10, 1263–1275.
- Poulsen, S.S., et al., 2017. Multi-walled carbon nanotube-physicochemical properties predict the systemic acute phase response following pulmonary exposure in mice. *PLoS One* 12, e0174167.
- Qu, X., et al., 2012. Nanotechnology for a safe and sustainable water supply: enabling integrated water treatment and reuse. *Acc. Chem. Res.* 46 (3), 834–843.
- Roco, M., 2011. The long view of nanotechnology development: the national nanotechnology initiative at 10 years. *J. Nanopart. Res.* 13 (2), 427–445.
- Saber, A.T., et al., 2012. Inflammatory and genotoxic effects of sanding dust generated from nanoparticle-containing paints and lacquers. *Nanotoxicology* 6, 776–788.
- Schlagenhauf, L., et al., 2015. Carbon nanotubes released from an epoxy-based nanocomposite: quantification and particle toxicity. *Environ. Sci. Technol.* 49 (17), 10616–10623.
- Smulders, S., et al., 2014. Toxicity of nanoparticles embedded in paints compared with pristine nanoparticles in mice. *Toxicol. Sci.* 141, 132–140.
- SUVA, 2018. *Grenzwerte am Arbeitsplatz 2011 (Occupational Exposure Limits 2011)*. Swiss Accident Insurance Funds (SUVA), Lucerne.
- Takagi, A., et al., 2008. Induction of mesothelioma in p53 +/– mouse by intraperitoneal application of multiwall carbon nanotube. *J. Toxicol. Sci.* 33, 105–116.
- Takanashi, S., et al., 2012. Carcinogenicity evaluation for the application of carbon nanotubes as biomaterials in rash2 mice. *Sci. Rep.* 2, 498.
- Wang, J., et al., 2014. Lung injury induced by TiO₂ nanoparticles depends on their structural features: size, shape, crystal phases, and surface coating. *Int. J. Mol. Sci.* 15 (912), 22258–22278.

- Warheit, D.B., et al., 2007. Pulmonary toxicity study in rats with three forms of ultrafine-TiO₂ particles: differential responses related to surface properties. *Toxicology* 230, 90–104.
- Weir, A., et al., 2012. Titanium dioxide nanoparticles in food and personal care products. *Environ. Sci. Technol.* 46 (4), 2242–2250.
- Wick, O., et al., 2007. The degree and kind of agglomeration affect carbon nanotube cytotoxicity. *Toxicol. Lett.* 168 (2), 121–131.
- Wick, P., et al., 2011. A brief summary of carbon nanotubes science and technology: a health and safety perspective. *ChemSusChem* 4, 905–911.
- Wittmaack, K., 2007. In search of the Most relevant parameter for quantifying lung inflammatory response to nanoparticle exposure: particle number, surface area, or what? *Environ. Health Perspect.* 115 (2), 187–194. <https://doi.org/10.1289/ehp.9254>.
- Wohlleben, W., et al., 2011. On the lifecycle of nanocomposites: comparing released fragments and their in-vivo hazards from three release mechanisms and four nanocomposites. *Small* 7, 2384–2395.
- Zimmerman, N., et al., 2015. A source-independent empirical correction procedure for the fast mobility and engine exhaust particle sizers. *Atmos. Environ.* 100, 178–184.